Resilience of orbital-angular-momentum photonic qubits and effects on hybrid entanglement

Daniele Giovannini,[1] Eleonora Nagali,[1] Lorenzo Marrucci,[2,3] and Fabio Sciarrino[1,4,*]

[1]*Dipartimento di Fisica, Sapienza Università di Roma, Roma I-00185, Italy*

[2]*Dipartimento di Scienze Fisiche, Università di Napoli Federico II, Complesso Universitario di Monte S. Angelo, I-80126 Napoli, Italy*

[3]*CNR-SPIN, Complesso Universitario di Monte S. Angelo, I-80126 Napoli, Italy*

[4]*Istituto Nazionale di Ottica (INO-CNR), Largo E. Fermi 6, Florence I-50125, Italy*

(Received 17 November 2010; published 29 April 2011)

The orbital angular momentum of light (OAM) provides a promising approach for the implementation of multidimensional states (qudits) for quantum-information purposes. In order to characterize the degradation undergone by the information content of qubits encoded in a bidimensional subspace of the orbital angular momentum degree of freedom of photons, we study how the state fidelity is affected by a transverse obstruction placed along the propagation direction of the light beam. Emphasis is placed on the effects of planar and radial hard-edged aperture functions on the state fidelity of Laguerre-Gaussian transverse modes and the entanglement properties of polarization-OAM hybrid-entangled photon pairs.

DOI: 10.1103/PhysRevA.83.042338 PACS number(s): 03.67.−a, 42.50.Ex, 42.50.Dv

I. INTRODUCTION

In quantum-information theory the fundamental unit of information is a two-level quantum system, the qubit. As in classical information science with bits, all quantum-information tasks can at least in theory be performed through just qubits and quantum gates operating on qubits [1–3]. For quantum-information purposes and the effective production and processing of robust qubits, as well as that of multidimensional quantum states or qudits [4,5], considerable interest has been recently focused on the generation and manipulation of helical laser beams. These optical waves, which have been shown to carry well-defined values of orbital angular momentum (OAM), are well described in terms of Laguerre-Gaussian (LG) modes, containing an ℓ-charged optical phase singularity (or optical vortex) at their beam axis [6–8]. Any two of such OAM modes with opposite values of ℓ and a common radial profile, here denoted as $|+\ell\rangle$ and $|-\ell\rangle$, define a basis of a bidimensional OAM subspace, $o_{|\ell|}$, in which one can encode a generic qubit. These specific OAM subspaces are particularly convenient to this purpose as they are not affected by propagation-induced decoherence, because the radial profile factorizes and can be usually ignored [9]. Experimentally, single-photon qubits in the OAM subspace o_2 can be efficiently encoded and readout by means of "polarization-OAM transferrers" [10,11], which are devices based on a recently introduced optical element called the "q-plate" [12].

The growing number of works demonstrating simple quantum-information protocols based on OAM-encoded qubits raise questions about how practical such an approach is, as compared, for instance, with the standard polarization encoding. For example, one can ask how sensitive are these OAM-encoded qubits to small optical misalignments or other nonideality of typical setups. More in general, studies of the resilience of OAM-encoded qubits or qudits in free-space propagation under the effect of perturbations and of imperfect detection are pivotal for the use of the OAM of light for quantum communication tasks. Previous works on LG modes in the classical regime showed, for example, the spread of measured transverse modes when planar restrictions spanning an angular range of less than 2π are placed along the beam [13,14], the consequences of noncoaxial mode detection [15], and the effect of turbulence on OAM-encoded information [16–21].

The purpose of this paper is to characterize the degradation undergone by the information encoded in o_2 OAM qubits when transverse hard-edged optical apertures are placed along the propagation direction of the beam, both in the classical and quantum regimes. The apertures considered in this work have one of the two shapes shown in Fig. 1, which are here taken to mimic the typical effect of optical misalignments or of the finite numerical aperture of optical components.

This paper is organized as follows: Section II introduces a classical theoretical model, based on the functional shape of LG modes, used to assess the degradation undergone by states belonging to three different o_2 bases as a consequence of the perturbation introduced during propagation by the two kinds of optical apertures. In Sec. III, we compare the theoretical predictions with the results of experiments performed in the classical regime. In Sec. IV, we finally present the experimental results concerning the effects of the previously introduced obstructions on the entanglement properties of a hybrid polarization-OAM entangled pair of twin photons [22,23], that is, a pair of entangled photons whose entanglement is encoded in two different degrees of freedom.

II. THEORY

An OAM eigenstate, $|\ell\rangle$, is here taken to denote a pure LG mode, corresponding to the wave function $A(x,y,z) = A(r,\phi,z) = A_0(r,z)\,e^{i\ell\phi}$ with azimuthal index ℓ, where z is the propagation axis; x,y are the Cartesian coordinates for the transverse plane; and r,ϕ are the corresponding polar coordinates. LG modes are characterized also by another index, p, determining the radial profile. In the following, except where explicitly stated otherwise, this radial index is understood to be $p = 0$ and is omitted.

*fabio.sciarrino@uniroma1.it

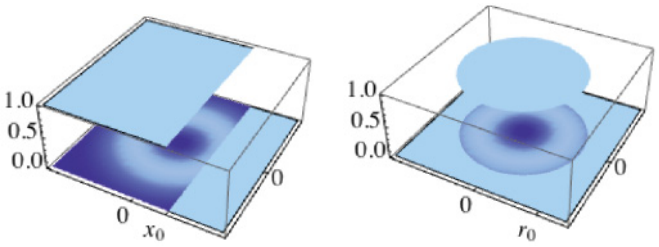

(a) $B(x_0, x; y)$ (b) $\Pi(r_0, r; \phi)$

FIG. 1. (Color online) Aperture functions: (a) planar transverse obstruction $B(x_0,x; y)$ (knife), and (b) radial obstruction $\Pi(r_0,r; \phi)$ (iris).

Generic OAM qubits are described by superpositions $|\psi\rangle = \alpha|+2\rangle + \beta|-2\rangle$, where α and β are complex coefficients. We consider, in particular, the following six representative states, belonging to three mutually unbiased bases of the OAM subspace o_2: $|l\rangle = |+2\rangle$, $|r\rangle = |-2\rangle$; $|h\rangle = (|l\rangle + |r\rangle)/\sqrt{2}$, $|v\rangle = -i(|l\rangle - |r\rangle)/\sqrt{2}$; and $|d\rangle = (1-i)(|l\rangle + i|r\rangle)/2$, $|a\rangle = (1+i)(|l\rangle - i|r\rangle)/2$ [24]. The wave functions $A(x,y,z)$ of these states are given by the corresponding superpositions of pure LG modes. All input wave functions are normalized for integration in any given (arbitrary) transverse plane z of the beam, i.e., $\int\int |A|^2 dx\, dy = 1$.

As mentioned in the Introduction, we consider two sets of optical apertures: (i) a half-plane obstruction with its edge located at the variable abscissa x_0, described by the transmittance function $B(x_0,x; y) = \theta(x_0 - x)$, where $\theta(x)$ is the Heaviside step function [see Fig. 1(a)]; and (ii) an iris with variable aperture radius r_0, described by the transmittance function $\Pi(r_0,r;\phi) = \theta(r_0 - r)$ [see Fig. 1(b)]. The first kind of aperture is meant to mimic the perturbations arising from small transverse optical misalignments, while the second corresponds to introducing optical elements having a small numerical aperture.

Now, given an arbitrary input qubit, $|\psi\rangle$, as described by the wave function A, the perturbed state $|\psi'\rangle$ obtained immediately after the aperture is given by the (not normalized) wave function $A' = AB$ or $A' = A\Pi$, respectively [see, e.g., Figs. 2(a) and 2(b)]. Given the normalization of the input wave function, the transmitted fraction of photons after the aperture is given by $T = \int\int |A'|^2 dx\, dy$. We then introduce the following two projections:

$$\kappa_\psi = \int_{-\infty}^{\infty} dx \int_{-\infty}^{\infty} dy\; A^*(x,y)\; A'(x,y) \tag{1a}$$

$$\kappa_{\psi^\perp} = \int_{-\infty}^{\infty} dx \int_{-\infty}^{\infty} dy [A^\perp(x,y)]^* A'(x,y), \tag{1b}$$

where $A^\perp$ is the wave function of the orthogonal state within the o_2 OAM subspace (with $p = 0$). We take the final detection probability of states ψ and $\psi^\perp$ to be given by $P(\psi) = |\kappa_\psi|^2$ and $P(\psi^\perp) = |\kappa_{\psi^\perp}|^2$, respectively. Therefore, $P_{o_2} = |\kappa_\psi|^2 + |\kappa_{\psi^\perp}|^2$ represents the probability of information preservation in the OAM subspace o_2 (with $p = 0$) after the initial mode has been transmitted through the aperture. The complementary fraction $1 - P_{o_2}$ of photons is lost either because they are absorbed in the aperture (as given by the fraction $1 - T$) or because they are transferred out of the $o_2 p = 0$ subspace and therefore are finally filtered out by the measurement process (note that this implies that the detection optics is assumed to have a small numerical aperture, thus strongly favoring $p = 0$ over higher radial modes). The computed OAM spectrum broadening induced by the planar aperture (function B) is shown in Fig. 3, for different positions of the aperture as specified by the resulting transmittance T.

The detected photons, however, will transport a partially degraded OAM qubit. The amount of quantum-information content that can be reconstructed by a receiver by means of projective measurements can be described through a fidelity parameter F defined as $F = P(\psi)/[P(\psi) + P(\psi^\perp)]$.

For each OAM state $|\psi\rangle$ and each position x_0 (or radius r_0) of the obstruction, the probabilities $P(\psi)$ and $P(\psi^\perp)$ were computed using numerical integration. The corresponding predictions for the information-preservation probability P_{o_2} are shown in Fig. 4, together with the corresponding mode profiles.

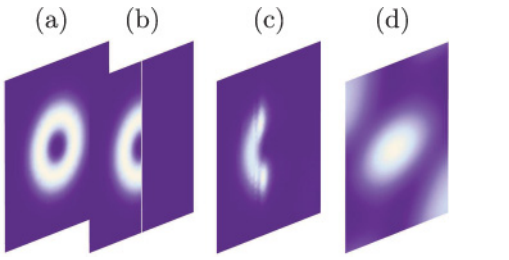

FIG. 2. (Color online) Propagation of an $LG_{0,+2}$ beam (basis state $|l\rangle$) through a $B(x_0)$ aperture function with $T = 0.5$. Profiles are drawn to the same scale. From left to right: (a) unperturbed transverse intensity profile; (b) intensity profile immediately after the aperture function (0.01 nm from the obstruction); (c) calculated profile after free-space propagation of the perturbed mode for $d = 30$ cm after the obstruction; (d) calculated profile after the insertion of a q-plate optical element (see Ref. [12]), used for the conversion into a TEM_{00} mode after the propagation of $d = 30$ cm.

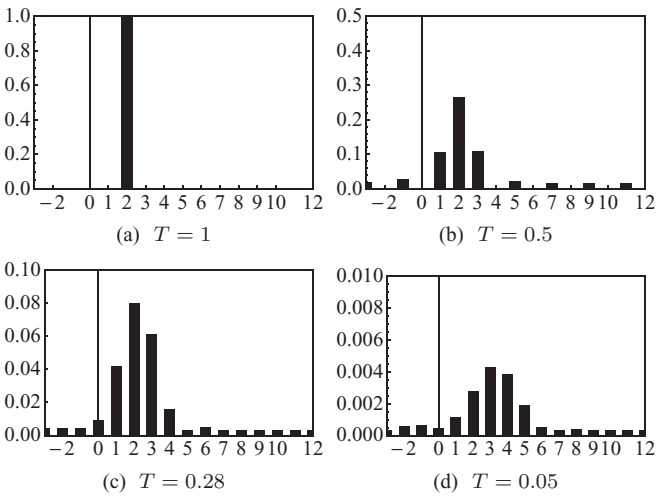

FIG. 3. (Color online) Spread in the measurement probabilities of OAM modes with $\ell' = -2, \ldots, 12$ for various positions x_0 of a $B(x_0)$ aperture inserted into the path of an $\ell = 2$ beam (i.e., for decreasing values of transmittance T).

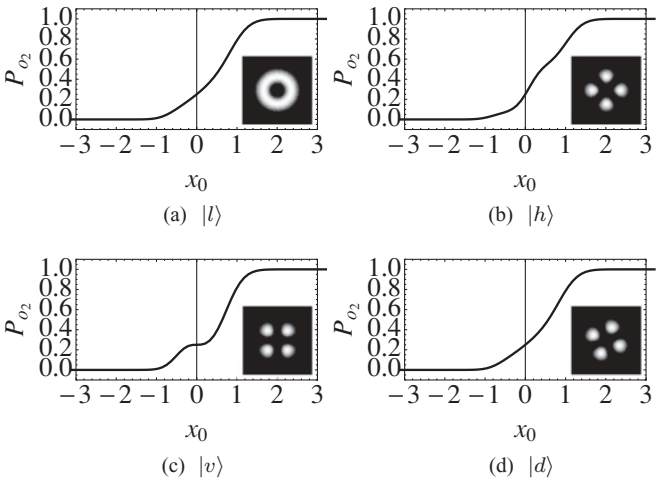

FIG. 4. (Color online) Theoretical curves of P_{o_2} for aperture function $B(x_0)$ for input states $|l\rangle$ ($|r\rangle$ exhibits the same curve), $|h\rangle$, $|v\rangle$, and $|d\rangle$ (or $|a\rangle$). The aperture edge position x_0 is given in units of the beam waist w_0). The mode intensity profile of each state is also shown in the inset of each panel. The aperture edge is vertically oriented in the inset frames.

The computed mean-information-preservation probability P_{o_2} and fidelity F for the aperture function $B(x_0)$, averaged over the six OAM states, are shown in Fig. 5 as solid lines. The mean P_{o_2} relative to the aperture function $P(r_0)$ is shown in Fig. 6. The theoretical fidelity in this second case is constantly unitary, because the rotational symmetry is not broken by the aperture.

III. CLASSICAL EXPERIMENTS

Classical measurements were performed on coherent beams by generating the OAM modes in o_2 corresponding to the six

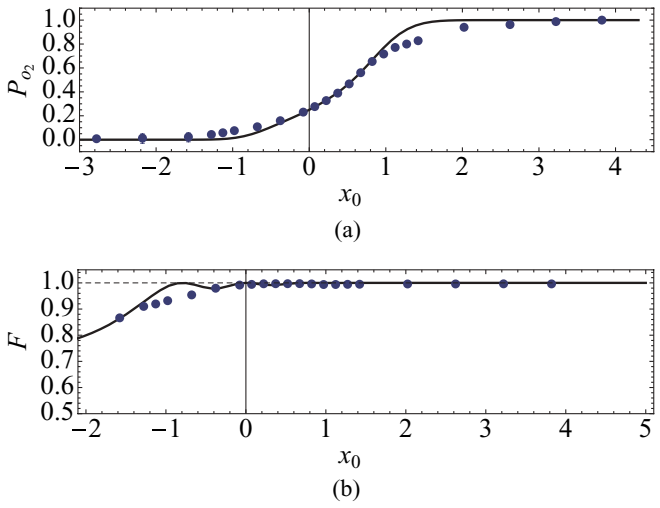

FIG. 5. (Color online) Average information-preservation probability P_{o_2} (a) and fidelity (b) for planar aperture function $B(x_0)$: lines are theoretical predictions, circles are data obtained in classical measurements (average over states $|d\rangle$ and $|a\rangle$), and experimental errors are negligible. The aperture edge position x_0 is given in units of the beam waist w_0).

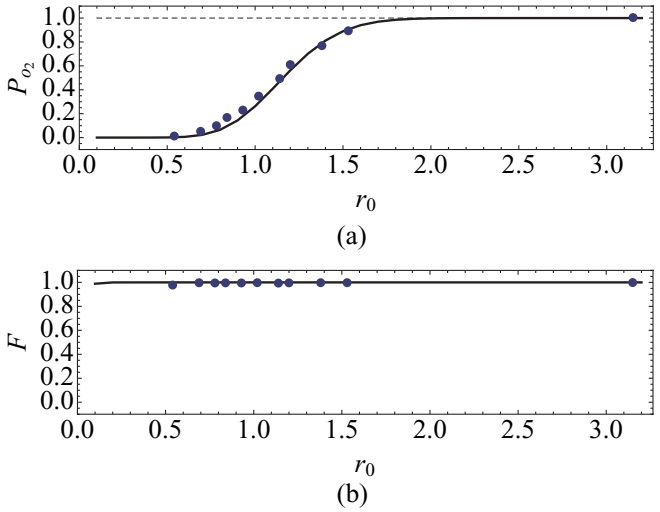

FIG. 6. (Color online) Average information-preservation probability P_{o_2} (a) and fidelity (b) for circular aperture function $\Pi(r_0)$: lines are theoretical predictions, and circles are data obtained in classical measurements, as a function of the aperture radius r_0 in units of the beam waist w_0.

states ($|l\rangle$, $|r\rangle$), ($|h\rangle$, $|v\rangle$, $|d\rangle$, $|a\rangle$) and then placing either a knife (aperture function B) or an iris (function Π) along the beam path. The perturbed modes $|\psi'\rangle$ were then projected onto $|\psi\rangle$ and $|\psi^{\perp}\rangle$ by the analysis setup. We assumed that no significant degradation (except possibly for some additional small losses) occurs to the quantum information in the analysis setup.

In the experimental implementation, a continuous laser beam was coupled to a single-mode fiber in order to collapse its transverse spatial mode into a pure TEM_{00}, corresponding to OAM $\ell = 0$. After the fiber, a polarization set was used to prepare the input polarization state as one of the six qubits. The beam was then sent through a quantum transferrer, $\pi \rightarrow o_2$, which transferred the polarization quantum state to the OAM degree of freedom, thus obtaining one of the input OAM state to be studied [9,10]. In order to analyze with high efficiency the OAM state after the aperture, we then exploited an inverse $o_2 \rightarrow \pi$ transferrer and a polarization analysis set [9]. The inverse transferrer includes the coupling to a single-mode fiber, which in our case was achieved with a typical efficiency $\eta = 14.8\%$. Although the q-plate device used in the transferrers is known to generate a radial profile more complex than a pure LG mode [25], only the $p = 0$ radial modes will be efficiently coupled to the final single-mode fiber used in our analysis setup, so that the $p = 0$ assumption used in our theory appears to be well justified.

The experimental average data for aperture B and states $|d\rangle$ and $|a\rangle$ are shown in Fig. 5, and those for Π and all o_2 basis states are shown in Fig. 6.

A comparison between the theoretical curves and the experimental points in Figs. 5, 6, and 7 shows a good quantitative agreement. Indeed, as highlighted in Fig. 7, even when the position of the obstruction causes a significant decrease of the transmittance, the state fidelity remains always above 90%. This demonstrates that, even in a high-loss regime, the initial information content encoded in the unperturbed state is preserved in the given OAM subspace even if a significant

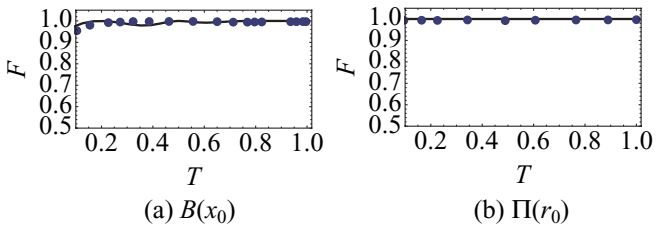

FIG. 7. (Color online) Fidelities versus transmittance in the classical regime for the two aperture geometries: theoretical predictions (solid lines) and experimental data (circles).

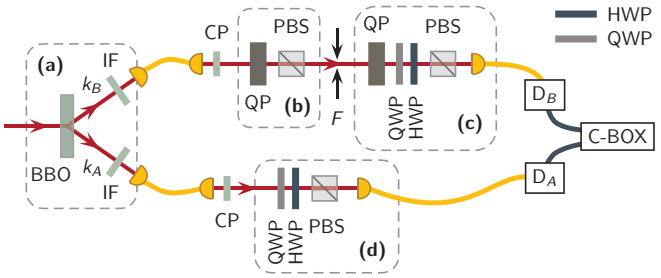

FIG. 8. (Color online) Experimental setup for the generation of hybrid polarization-OAM entangled photon pairs, with the application of the aperture function F. (a) Generation of polarization-entangled photons on modes k_A and k_B. (b) Encoding of the state of one photon in the OAM subspace o_2 through the $\pi \rightarrow o_2$ transferrer. (c) OAM analysis. (d) Polarization analysis.

spread of the initial OAM spectrum takes place (see Fig. 3). Any discrepancies may be explained by an imperfect mode generation and, more appreciably, by a higher sensitivity to small fluctuations of the fidelity parameter when T approaches zero. This result shows that the information content of OAM qubits exhibits a remarkable resilience to perturbations such as those examined here.

In particular, the reported high fidelities correspond to the experimental fact that after the aperture one still has $|\kappa_{\psi^\perp}|^2 \ll |\kappa_\psi|^2$. This result is tied to the moderate spread of the OAM spectrum of the perturbed state even for low values of T and the progressive shift of the central spectral state when the initial mode is almost completely blocked, as shown in Fig. 3.

The present work focuses on qubits encoded in the bidimensional o_2 subspace. However, it is worth noting that higher-order subspaces o_k, with LG basis states $\{|+k\rangle, |-k\rangle\}$, are likely to offer higher and higher resilience, the higher the OAM winding number k (while we may expect a lower resilience in the o_1 subspace). Indeed, as shown in Fig. 3 for the $|\ell| = 2$ case, the increased distance $\Delta\ell$ between the two orthogonal basis states causes the spread of the detection probabilities around a perturbed basis state $|+k\rangle$ to have a decreasing overlap with $|-k\rangle$ as k increases. Therefore, while the information-preservation probability is strongly affected, the fidelity is expected to remain high even for very low transmittance. Of course, these results do not apply to other subspaces of OAM not involving opposite values of the OAM eigenvalue, so it remains to be seen whether the same resilience can be achieved for OAM qudits. Our results are also in qualitative agreement with former investigations on the OAM spectrum broadening occurring for LG beams passing through variable angular optical apertures [26,27].

IV. RESILIENCE OF HYBRID POLARIZATION-OAM ENTANGLEMENT

After the classical regime experiments, we moved to a quantum regime. We are specifically interested in evaluating the resilience of the entanglement involving the OAM degree of freedom of a photon, under the effect of an optical aperture. In particular, we have considered the case of a planar aperture [function $B(x_0)$] inserted in the path of a photon belonging to photon pair that is initially prepared in a hybrid-entangled state of OAM and polarization. The choice of using hybrid entanglement is mainly practical, as we start from a polarization-entangled pair of photons and then the quantum state of one of the two photons is transferred into the OAM by using a polarization-OAM transferrer, as recently reported in [22].

Polarization-entangled photon pairs were created by spontaneous parametric down-conversion; the spatial profile of the twin photons was filtered through single-mode fibers, and the polarization state of one of them was coherently transferred to the corresponding OAM state. The aperture was then used to perturb the photon carrying the OAM entangled information and, finally, the two-photon quantum state was analyzed and the fidelity with the initially prepared state was computed. The experimental arrangement, shown in Fig. 8, is analogous to that adopted in the high-quality generation of hybrid polarization-OAM entangled photon pairs in [22], and it extends to the case of entangled photon pairs in the setup used in the previous section. A 1.5-mm-thick β-barium borate crystal (BBO) cut for type-II phase matching was pumped by the second harmonic of a Ti:sapphire mode-locked laser beam. Via spontaneous parametric fluorescence, the BBO generated polarization-entangled photon pairs on modes k_A and k_B with wavelength $\lambda = 795$ nm and pulse bandwidth $\Delta\lambda = 4.5$ nm, as determined by two interference filters (IF). The spatial and temporal walk-off was compensated by inserting a $\lambda/2$ wave plate and a 0.75-mm-thick BBO crystal on each output mode k_A and k_B [28]. The source thus generated photon pairs in the polarization-encoded singlet entangled state, i.e., $\frac{1}{\sqrt{2}}(|H\rangle_A|V\rangle_B - |V\rangle_A|H\rangle_B)$.

The photon in mode k_A was sent through a standard polarization analysis setup and then coupled to a single-mode fiber connected to the single-photon counter modules D_A. The photon in mode k_B was coupled to a single-mode fiber, in order to collapse its transverse spatial mode into a pure TEM_{00} ($\ell = 0$). After the fiber output, two wave plates compensated the polarization rotation introduced by the fiber (CP). To transform the polarization-entangled pairs into a hybrid-entangled state, photon B was sent through the quantum transferrer $\pi \rightarrow o_2$, which converted the polarization quantum states into the corresponding OAM states. After the transferrer operation the polarization-entangled state was transformed into the hybrid entangled state $\frac{1}{\sqrt{2}}(|H\rangle_\pi^A|+2\rangle_{o_2}^B - |V\rangle_\pi^A|-2\rangle_{o_2}^B)$. After the aperture F, the inverse $o_2 \rightarrow \pi$ transferrer and a polarization analysis set was used to analyze

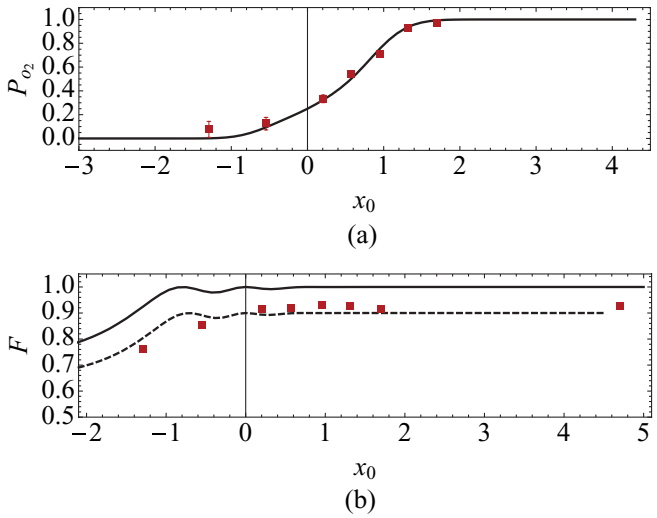

FIG. 9. (Color online) Information-preservation probability P_{o_2} (a) and fidelity (b) of the polarization-OAM hybrid-entangled pair of photons as a function of the planar aperture edge position x_0, given in units of the beam waist w_0: theoretical predictions (continuous line) and the one rescaled by the maximum value of measured fidelity (dashed line) compared to experimental data (squares).

the OAM photon state. Ultimately, the photon was coupled to a single-mode fiber and then detected by D_B, connected to the coincidence box (CB), which recorded the coincidence counts $\{D_A, D_B\}$.

The experimental results for the probability P_{o_2} and the fidelity F are shown in Fig. 9. We observed that the state fidelity achieves somewhat lower values than what was predicted (and than what was obtained for the classical experiment case), particularly when the aperture blocked more than half of the beam. It is clear from the figure that the fidelity reduction cannot be entirely ascribed to the aperture, as it remains constant even when the aperture is moved completely off the beam. The maximum fidelity of the two-photon state is presumably decreased by imperfections in the source, preparation, and measurement stages, to which it is typically more sensitive than in the single photon state. To account for this effect, we plotted the expected theoretical curves rescaled by the maximum value of measured fidelity. This rescaled curve exhibits a reasonable agreement with the experimental data [dashed line in Fig. 9(b)].

V. CONCLUSIONS

In this paper we tested the robustness of OAM-encoded qubits, which provide a useful and versatile quantum-communication resource. In the classical case, we first demonstrated that the information encoded in a bidimensional subspace of the OAM can be retrieved probabilistically in the same subspace even if the state is highly perturbed in such a way as to block a significant fraction of the transverse extension of the mode. The experimental results are in good agreement with the theoretical model.

We then proceeded to demonstrate also in the single-photon regime, by using polarization-OAM entangled photon pairs, the high resilience of single-photon bidimensional OAM states. We verified that hybrid entanglement correlations persist even in high-loss conditions.

ACKNOWLEDGMENTS

This work was supported by Project HYTEQ-FIRB, Finanziamento Ateneo 2009 of Sapienza Università di Roma, and European Project PHORBITECH of the FET Program (Grant No. 255914).

[1] M. A. Nielsen and I. L. Chuang, *Quantum Computation and Quantum Information* (Cambridge University Press, Cambridge, UK, 2000).
[2] N. Gisin, G. Ribordy, W. Tittel, and H. Zbinden, Rev. Mod. Phys. **74**, 145 (2002).
[3] J. L. O'Brien, Science **318**, 1567 (2007).
[4] E. Nagali, L. Sansoni, L. Marrucci, E. Santamato, and F. Sciarrino, Phys. Rev. A **81**, 052317 (2010).
[5] E. Nagali, D. Giovannini, L. Marrucci, S. Slussarenko, E. Santamato, and F. Sciarrino, Phys. Rev. Lett. **105**, 073602 (2010).
[6] A. Mair, V. Alipasha, G. Weihs, and A. Zeilinger, Nature (London) **412**, 313 (2001).
[7] G. Molina-Terriza, J. P. Torres, and L. Torner, Nat. Phys. **3**, 305 (2008).
[8] S. Franke-Arnold, L. Allen, and M. Padgett, Laser Photonics Rev. **2**, 299 (2008).
[9] E. Nagali *et al.*, Opt. Express **17**, 18745 (2009).
[10] E. Nagali, F. Sciarrino, F. De Martini, L. Marrucci, B. Piccirillo, E. Karimi, and E. Santamato, Phys. Rev. Lett. **103**, 013601 (2009).
[11] E. Nagali *et al.*, Nat. Photonics **3**, 720 (2009).
[12] L. Marrucci, C. Manzo, and D. Paparo, Phys. Rev. Lett. **96**, 163905 (2006).
[13] J. Arlt, J. Mod. Opt. **50**, 1573 (2003).
[14] G. Gibson *et al.*, Opt. Express **12**, 5448 (2004).
[15] M. V. Vasnetsov, V. A. Pas'ko, and M. S. Soskin, New J. Phys. **7**, 46 (2005).
[16] C. Paterson, Phys. Rev. Lett. **94**, 153901 (2005).
[17] C. Gopaul and R. Andrews, New J. Phys. **9**, 94 (2007).
[18] G. Gbur and R. K. Tyson, J. Opt. Soc. Am. A **25**, 225 (2008).
[19] B. J. Pors, C. H. Monken, E. R. Eliel, and J. P. Woerdman, Opt. Expr. **19**, 6671 (2011).
[20] G. A. Tyler and R. W. Boyd, Opt. Lett. **34**, 142 (2009).
[21] A. A. Semenov and W. Vogel, Phys. Rev. A **81**, 023835 (2010).
[22] E. Nagali and F. Sciarrino, Opt. Express **18**, 18243 (2010).

[23] E. Karimi, J. Leach, S. Slussarenko, B. Piccirillo, L. Marrucci, L. Chen, W. She, S. Franke-Arnold, M. J. Padgett, and E. Santamato, Phys. Rev. A **82**, 022115 (2010).
[24] M. J. Padgett and J. Courtial, Opt. Lett. **24**, 430 (1999).
[25] E. Karimi, B. Piccirillo, L. Marrucci, and E. Santamato, Opt. Lett. **34**, 1225 (2009).
[26] A. K. Jha, B. Jack, E. Yao, J. Leach, R. W. Boyd, G. S. Buller, S. M. Barnett, S. Franke-Arnold, and M. J. Padgett, Phys. Rev. A **78**, 043810 (2008).
[27] B. Jack *et al.*, New J. Phys. **11**, 103024 (2009).
[28] P. G. Kwiat, E. Waks, A. G. White, I. Appelbaum, and P. H. Eberhard, Phys. Rev. A **60**, R773 (1999).